JOURNAL OF COMPUTATIONAL PHYSICS 20, 268–278 (1976)

A General Finite-Difference Formulation with Application to Navier–Stokes Equations*

JOHN C. CHIEN

ARO, Incorporated, Arnold Air Force Station, Tennessee 37389

Received February 27, 1975; revised June 6, 1975

A general method for deriving a finite-difference equation from a partial differential equation with the use of local model solutions is presented. The method, which is based on the evaluation of local functions, is illustrated by applying to a time-dependent vorticity equation. The main advantage of the present approach is that there is no apparent stability limitation on grid size and time step. Time dependent Navier–Stokes equations are solved with the present formulation for a Couette flow with constant suction and a square cavity flow problems. Steady-state, convergent solutions are obtained with grid sizes and time steps much larger than those determined from the conventional stability criteria for the forward time central difference method. The local model solutions used in the present paper were designed to produce steady-state solution; care must be taken to interpret the transient solution obtained from the present model with large time step.

1. INTRODUCTION

It is well known that certain criteria determining numerical stability must be taken into account when performing finite-difference calculation of a general class of flow problems [1, 2]. These limitations on grid sizes and time steps are directly related to the discretization errors associated with the derived finite-difference equation. The problem of the discretization error and the numerical stability can be minimized or eliminated if one can make use of local analytical model solutions of the governing partial-differential equation in the formulation of a finite-difference equation. For example, a partial-differential equation can be written as

$$L\{\phi\} = 0, \tag{1}$$

* The research reported herein was sponsored by the Arnold Engineering Development Center, Air Force Systems Command, Arnold Air Force Station, Tennessee. The results were obtained by ARO, Inc. (a subsidiary of Sverdrup and Parcel and Associates, Inc.), contract operator of AEDC. Further reproduction is authorized to satisfy needs of the U. S. Government.

where L is a differential operator. Equation (1) written in a conventional finite-difference form is

$$L_f\{\phi\} = \epsilon, \tag{2}$$

where L_f is a finite-difference operator and ϵ represents the difference

$$\epsilon = L\{\phi\} - L_f\{\phi\}. \tag{3}$$

In the present approach, the finite-difference equation for Eq. (1) is written as

$$L_f\{\phi, G^*\} = 0, \tag{4}$$

where the additional function G^* is introduced to eliminate the error ϵ. The remaining problem is then to determine the function G^*. Since local analytical solutions for multi-dimensional problems may be lengthy and tedious to evaluate, a one-dimensional model is used in the present analysis to obtain approximate function G instead of the exact function G^*. The name of the "decay function" is used for G or G^* in the present analysis. Equation (4) now can be written as

$$L_f\{\phi, G\} = \Delta. \tag{5}$$

The above equation is a general form of the present formulation.

2. One-Dimensional Example

The procedure is best illustrated for the following time-dependent vorticity equation.

$$\frac{\partial \Omega}{\partial t} = \nu \frac{\partial^2 \Omega}{\partial y^2} - v \frac{\partial \Omega}{\partial y}, \tag{6}$$

where Ω is the vorticity, ν is the kinematic viscosity, and v is the velocity. In the present approach, modified finite difference expressions are given as

$$\begin{aligned}
\frac{\partial \Omega}{\partial t} &\approx \frac{\Omega_j^{n+1} - \Omega_j^{n}}{\delta t} \cdot \frac{1}{G_t}, \\
\frac{\partial^2 \Omega}{\partial y^2} &\approx \frac{\Omega_{j+1}^{n} - 2\Omega_j^{n} + \Omega_{j-1}^{n}}{\delta y^2} \cdot \frac{1}{G_j}, \\
\frac{\partial \Omega}{\partial y} &\approx \frac{\Omega_{j+1}^{n} - \Omega_{j-1}^{n}}{2\delta y} \cdot \frac{1}{F_j},
\end{aligned} \tag{7}$$

where the subscript represents the gridpoint and the superscript represents the time step. With Eq. (7), the resulting finite difference equation becomes

$$\frac{\Omega_j^{n+1} - \Omega_j{}^n}{\delta t} \cdot \frac{1}{G_t} = \nu \left\{ \frac{\Omega_{j+1}^n - 2\Omega_j{}^n + \Omega_{j-1}^n}{\delta y^2} \cdot \frac{1}{G_j} - \left(\frac{v}{\nu}\right)_j \frac{\Omega_{j+1}^n - \Omega_{j-1}^n}{2\delta y} \right\}. \quad (8)$$

The function F_j is not explicitly used in Eq. (8) because two functions are actually needed for the Eq. (6), which has only three terms in it. Equation (8) can be arranged to provide an explicit formula for the calculation of Ω_j^{n+1} in terms of Ω_{j+1}^n, Ω_{j-1}^n, $\Omega_j{}^n$, grid size (δy), time step (δt), and the decay functions G_t and G_j. Note that with $G_t = 1$ and $G_j = 1$, Eq. (8) reduces to the conventional forward time central difference formula (FTCD). Two well-known numerical stability limitations exist that limit the time step δt and the grid size δy, i.e.,

$$R_j \equiv \frac{v\,\delta y}{\nu} \leqslant 2, \qquad S \equiv \frac{\nu\,\delta t}{\delta y^2} \leqslant \frac{1}{2}. \quad (9)$$

In principle, one can always use smaller grid sizes and time steps and carry out the numerical computation for a longer time, but often, one is limited by the computing time and storage available. Besides, one is often more interested in the steady-state solution rather than the transient solution, even though the time dependent approach is used.

The purpose of the present analysis then, is to provide a method that enables one to obtain a stable and accurate solution with larger grid sizes and time steps. With this in mind, we now proceed forward to determine the decay function G_t and G_j.

To determine G_j, decouple the right-hand side of Eq. (8) from the left-hand side. This is done simply by making a "quasi-steady state" assumption, i.e., locally, in time $\partial/\partial_t \approx 0$. This is not a trivial assumption because a local analytical steady-state solution can exist. The decay function G_j can be obtained by comparing the local finite-difference solution with the local analytical steady-state model solution. In the derivation, v and $\Omega_{j\pm1}$ values are assumed constant. The result is

$$G_j = \frac{2}{R_j}\left(1 - \frac{2(e^{R_j} - 1)}{e^{2R_j} - 1}\right). \quad (10)$$

The use of the local steady-state model solution also can be found in the classical paper by Allen and Southwell [3] and Spalding [4]. The function G_j is shown in Fig. 1. Often, an approximate form of the decay function G_j is desirable to save

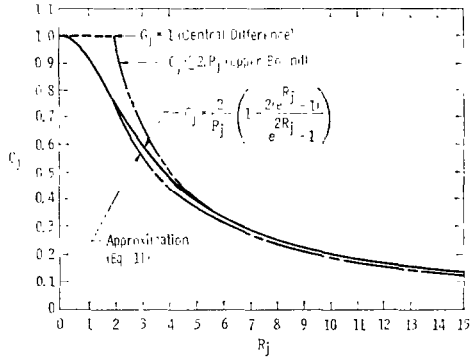

FIG. 1. Spatial decay function G_j

the computing time in evaluating the exponential functions in Eq. (10). One such approximate form is given here

$$\begin{aligned} G_j &= 1.0 - 0.0625 \cdot (R_j)^2, && |R_j| < 2.0, \\ &= \frac{2}{|R_j|} - \frac{1}{(R_j)^2}, && |R_j| \geqslant 2.0. \end{aligned} \tag{11}$$

The determination of the time decay function G_t requires a local time-dependent analytical solution to a model equation. The model equation is derived from Eq. (6) based on an explicit scheme, i.e., Ω_j^{n+1} at the $(n+1)$th time step can be explicitly determined from Ω_j^n, Ω_{j+1}^n, and Ω_{j-1}^n at the nth time step. By substituting the finite difference expressions for the spatial derivatives in Eq. (6), one can formulate an explicit time-dependent model equation for Ω_j as

$$(\partial \Omega_j/\partial t) + 2C \cdot \Omega_j = 2C \cdot E^n, \tag{12}$$

where

$$C = \nu\, \delta t/(\delta y^2 \cdot G_j),$$

$$E^n = \{\Omega_{j-1}^n + (\Omega_{j+1}^n - \Omega_{j-1}^n) \cdot (1 - R_j \cdot G_j/2)/2\}.$$

The time integration of Eq. (12) from the nth time step to the $(n+1)$th time step gives

$$\Omega_j^{n+1} = \Omega_j^n \cdot e^{-2C} + (1 - e^{-2C}) \cdot E^n, \qquad \text{with} \quad \Omega_{j\pm 1}^n = \text{const.} \tag{13}$$

By comparing the finite-difference Eq. (8) and the local time-dependent solution (13), the decay function G_t can be determined.

$$G_t = (1 - e^{-2C})/2C. \tag{14}$$

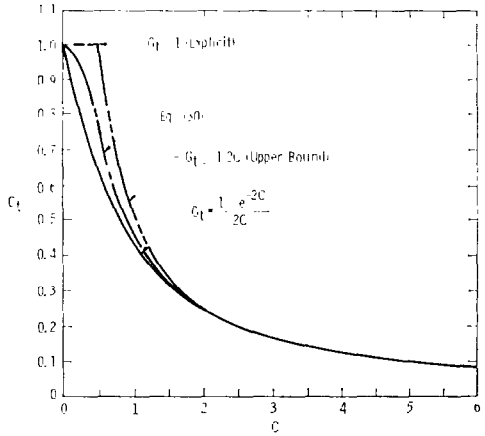

FIG. 2. Time decay funtion G_t

The time decay function G_t is shown in Fig. 2. To reduce computing time, an approximate form of G_t is given as

$$G_t = \frac{1}{2(C+1)} + \frac{1}{2(C+1)^2}. \tag{15}$$

With the decay function G_j and G_t determinated by the present method, the next important point is to determine if the formulation provides a stable solution for larger time steps and grid sizes than those determined from Eq. (9) for the conventional formulation. It is not difficult to see that the present finite difference Eq. (8), with the decay functions given by Eqs. (10) and (14), converges to the original partial differential Eq. (6) as the grid size (δy) and time step (δt) goes to zero in the limit. The stability limitation of the Eq. (8) can be easily derived by redefining ν as $\nu G_t/G_j$ and v as vG_t in Eq. (9), i.e.,

$$1 - \frac{R_j \cdot G_j}{2} \geqslant 0, \qquad 1 - \frac{2S \cdot G_t}{G_j} \geqslant 0. \tag{16}$$

The condition (16) also provides upper bounds for the spatial decay function G_j and the time-wise decay function G_t, namely, $G_j \leqslant 2/R_j$ and $G_t \leqslant 1/2C$ (see Figs. 1 and 2).

For the conventional FTCD method, the decay functions G_j and G_t are set equal to unity. The stability limitation (9) is readily recovered from Eq. (16). The grid size and the time step for the FTCD method is thus limited by the Eq. (9). On the other hand, the condition given by Eq. (16) is automatically satisfied with decay functions given by Eqs. (10) and (14) for all values of R_j and S. There is

no apparent stability limitation on the grid size and the time step for the present formulation. This is the basic advantage of the present method over the conventional FTCD method. Therefore, large time steps and grid sizes can be used in the computation without suffering the numerical stability problem. This important characteristic of the present method will be further verified by applying it to various flow problems in the next section.

3. Application to Navier-Stokes Equations

To provide further evidence, Navier–Stokes equations are solved with the present formulation for two time-dependent, two-dimensional problems: (1) a Couette flow with constant suction through porous walls, (2) a square cavity flow with a moving wall.

3.1. *Time-Dependent Couette Flow with Constant Suction*

The flow field between two initially stationary parallel porous plates is established by injecting the fluid through the lower porous plate and moving the flow out of the upper plate at an equal rate. The upper porous plate is then suddenly set to motion at a constant speed. The subsequent flow field can be described by the following time-dependent Navier–Stokes equations written in terms of the vorticity (Ω) and the velocity components (u, v).

$$\frac{\partial \Omega}{\partial t} + u\frac{\partial \Omega}{\partial x} + v\frac{\partial \Omega}{\partial y} = \nu\left(\frac{\partial^2 \Omega}{\partial x^2} + \frac{\partial^2 \Omega}{\partial y^2}\right), \tag{17}$$

$$\frac{\partial^2 u}{\partial x^2} + \frac{\partial^2 u}{\partial y^2} = -\frac{\partial \Omega}{\partial y}, \tag{18}$$

$$\frac{\partial^2 v}{\partial x^2} + \frac{\partial^2 v}{\partial y^2} = \frac{\partial \Omega}{\partial x}. \tag{19}$$

The finite difference formulation of Eqs. (17)–(19) is given as

$$\frac{\Omega_{i,j}^{n+1} - \Omega_{i,j}^{n}}{\delta t} \cdot \frac{1}{G_t} + u_{i,j}\frac{\Omega_{i+1,j}^{n} - \Omega_{i-1,j}^{n}}{2\delta x} + v_{i,j}\frac{\Omega_{i,j+1}^{n} - \Omega_{i,j-1}^{n}}{2\delta y}$$

$$= \nu\left\{\frac{\Omega_{i+1,j}^{n} + \Omega_{i-1,j}^{n} - 2\Omega_{i,j}^{n}}{\delta x^2} \cdot \frac{1}{G_i} + \frac{\Omega_{i,j+1}^{n} + \Omega_{i,j-1}^{n} - 2\Omega_{i,j}^{n}}{\delta y^2} \cdot \frac{1}{G_j}\right\} \tag{20}$$

$$\frac{u_{i+1,j}^{n+1} + u_{i-1,j}^{n+1} - 2u_{i,j}^{n+1}}{\delta x^2} + \frac{u_{i,j+1}^{n+1} + u_{i,j-1}^{n+1} - 2u_{i,j}^{n+1}}{\delta y^2} = -\frac{\Omega_{i,j+1}^{n} - \Omega_{i,j-1}^{n}}{2\delta y}, \tag{21}$$

$$\frac{v_{i+1,j}^{n+1} + v_{i-1,j}^{n+1} - 2v_{i,j}^{n+1}}{\delta x^2} + \frac{v_{i,j+1}^{n+1} + v_{i,j-1}^{n+1} - 2v_{i,j}^{n+1}}{\delta y^2} = \frac{\Omega_{i+1,j}^{n} - \Omega_{i-1,j}^{n}}{2\delta x}, \tag{22}$$

where

$$G_i = \frac{2}{R_i}\left(1 - \frac{2(e^{R_i} - 1)}{e^{2R_i} - 1}\right), \qquad G_j = \frac{2}{R_j}\left(1 - \frac{2(e^{R_j} - 1)}{e^{2R_j} - 1}\right),$$
$$G_t = \frac{1 - e^{-2\tilde{C}}}{2\tilde{C}}, \tag{23}$$
$$\tilde{C} = \left(\frac{1}{\delta x^2 \cdot G_i} + \frac{1}{\delta y^2 \cdot G_j}\right) \cdot \nu\, \delta t.$$

R_i and R_j are local grid Reynolds numbers in x and y directions.

The initial and boundary conditions are:

$$\begin{aligned} &t = 0, \quad \Omega = U = 0, \quad v = 0.1, && \text{for the whole flow field,} \\ &t = 0^+, \quad U = 1.0, \quad \Omega = -2.0/\delta y, && \text{at the upper plate,} \\ t > 0, \quad &U = 1.0, \quad \Omega^{n+1} = -2(1.0 - U_p^n)/\delta y - \Omega_p^n, && \text{at the upper plate,} \\ &U = 0, \quad \Omega = -0.000454, && \text{at the lower plate,} \end{aligned} \tag{24}$$

where U_p and Ω_p are the velocity and the vorticity at one point away from the upper wall. The exact analytical value of the vorticity at the lower plate was used to minimize the unnecessary error due to the finite-difference treatment of boundary conditions. The boundary condition at the planes normal to the porous plate is given as

$$\partial\phi/\partial x = 0, \qquad \phi = \Omega, u, v. \tag{25}$$

Numerical computation was carried out for a computational size of 3×11 points with grid size $(\delta x, \delta y)$ set equal to a value of 0.1. A constant kinematic viscosity ($\nu = 0.01$) was also used. Equation (20) is then used to provide the vorticity field at the $(n + 1)$th time step and velocity Eqs. (21) and (22) are solved iteratively (20 iterations per time step for all cases). Identical steady-state solutions were obtained for six different time steps, namely, $\delta t = 0.1$, 0.2, 0.5, 1.0, 2.0, and 5.0.

The steady-state velocity and vorticity distributions are given in Figs. 3a and b. The agreement between the present result and the exact analytical solution is excellent. The time history of the wall vorticity for $\delta_t = 1.0$ is shown in Fig. 4. The explicit solution ($G_t = 1.0$) diverges and is included for comparison. The computing time (total CPU time) required to reduce the residual ratio at the wall to a value below 1×10^{-6} varied from 1.6 to 2.5 sec on IBM 370/165 machine.

3.2. *Time-Dependent Square Cavity Flow with a Moving Wall*

Square cavity flow problem has been investigated by several authors. Due to its simple geometry, the square cavity problem has been used to test various numerical schemes for the calculation of recirculating flows [5–9]. Since the steady-state

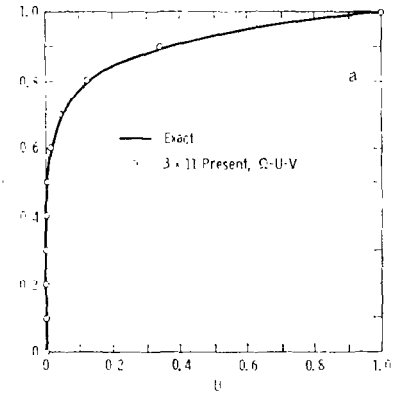

FIG. 3a. Steady-state velocity profile of the couette flow with constant suction,

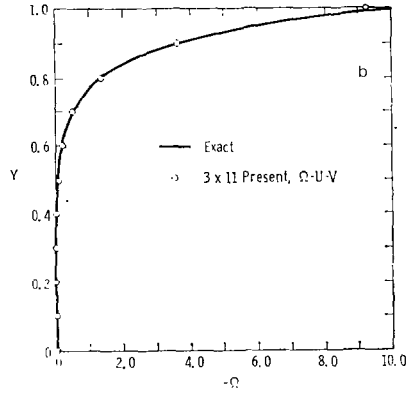

FIG. 3b. Steady-state vorticity profile of the couette flow with constant suction.

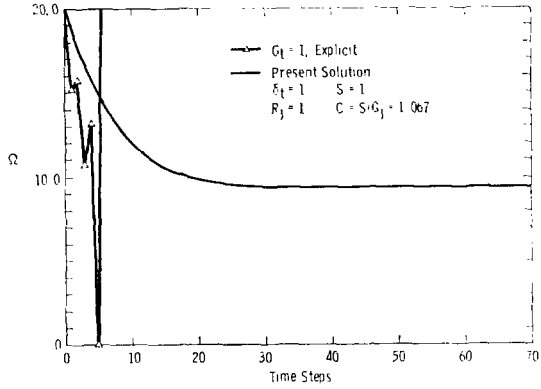

FIG. 4. Time history of the wall vocticity for couette flow problem

solutions are available in those previous investigations, it is selected as a test case for the present method. Initially, the flow in a square cavity is stationary. The upper wall is then set to motion at a constant speed U_0. The governing equations and the finite difference equations are the same as those given in Section 3.1. The initial and boundary conditions are:

$$t = 0,\ \Omega = U = v = 0, \qquad \text{for the whole flow field,}$$

$$t = 0^+,\ U = 1.0,\ \Omega = -2.0/\delta y,\ v = 0, \qquad \text{at the upper moving wall,}$$

$$t > 0,\ U = 1.0,\ \Omega^{n+1} = -2(1.0 - U_y{}^n)/\delta y - \Omega_y{}^n, \qquad \text{at the moving wall,}$$

$$U = V = 0,\ \Omega^{n+1} = -2U_y{}^n/\delta y - \Omega_y{}^n, \qquad \text{at the bottom wall,}$$

$$U = V = 0,\ \Omega^{n+1} = \pm 2V_x{}^n/\delta y - \Omega_x{}^n, \qquad \text{at the two side walls,}$$

where U_p, V_p, Ω_p are quantities evaluated at one point away from the corresponding wall. Two computational grid sizes are used in the calculation: one has 51×51 gridpoints ($\delta x = \delta y = 0.02$), the other has 11×11 grid points ($\delta x = \delta y = 0.1$). The time step is $\delta t = 1.0$ and the kinematic viscosity is 0.01 for both cases. Note that the time step used in the present calculation is much larger than those determined from Eq. (9) for conventional FTCD scheme, namely, $\delta t = 0.02$ for the 51×51 point case, and $\delta t = 0.5$ for the 11×11 point case. Steady-state convergent solutions are presented in Fig. 5 for the velocity distributions on the vertical center plane of the square cavity. The agreement with Burggraf's [5] 51×51 point solution is excellent. The present 11×11 point solution is also compatible with Mills [6] 15×15 point solution. To make sure that the present 11×11 point solution is consistent with the coarse grid size used, the same problem is solved in terms of a vorticity-stream function formulation ($\Omega - \psi$). The velocity Eqs. (18) and (19) are replaced by a single stream function equation.

$$\frac{\partial^2 \psi}{\partial x^2} + \frac{\partial^2 \psi}{\partial y^2} = -\Omega. \tag{26}$$

The stream function Eq. (26) is solved in a conventional central difference method with a zero stream function specified at the boundary walls. The steady-state solution of this vorticity-stream function formulation for a 11×11 point cavity is shown in Fig. 5. The agreement between the Ω–U–V solution and the Ω–ψ is good. It is concluded that the 11×11 point solution is consistent with the coarse grid size used. The computing time needed to reach a steady-state solution (residual $< 1 \times 10^{-5}$) for the 51×51 point case is about 7 min 30 sec. For the 11×11 point case, it took only 2.5 sec for the residual to reach a value below

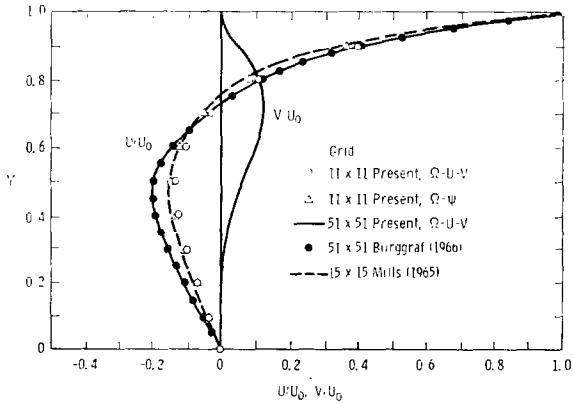

FIG. 5. Steady-state velocity profiles on the vertical center plane of a square cavity

1×10^{-6}. Note that 20 inner interations per time step are used throughout the test for the velocity cycle and the stream function cycle in all test cases to obtain convergent solutions within each time step. Although the number of inner iterations may be time and problem dependent, it was held constant so that the computing time to reach a steady-state solution can be easily compared.

3.3. *Inviscid Equation as Limiting Case of Infinite Reynolds Number*

As Reynolds number goes to infinity, the viscous equation (6) can be formally reduced to an inviscid equation outside the boundary layer region, i.e.,

$$\frac{\partial \Omega}{\partial t} = -v \frac{\partial \Omega}{\partial y}. \tag{27}$$

The large Reynolds number limit of the spatial decay function G_j can be easily derived from Eq. (11) as

$$G_j \approx \frac{2}{|R_j|}, \qquad |R_j| \to \text{infinity}. \tag{28}$$

With this limiting form of the decay function, the finite-difference equation (8) takes the following forms.

$$\begin{aligned} \frac{\Omega_j^{n+1} - \Omega_j^n}{\delta t} \cdot \frac{1}{G_t} &= -v \cdot \frac{\Omega_j^n - \Omega_{j-1}^n}{\delta y}, \qquad v > 0, \\ &= +v \cdot \frac{\Omega_{j+1}^n - \Omega_j^n}{\delta y}, \qquad v < 0. \end{aligned} \tag{29}$$

By simply looking at Eqs. (27) and (29), it is not difficult to see that the convection term is now represented by a two-point one-side upwind difference formula.

3.4. *Modified Decay Function Formula*

To simplify the computational effort, a proposed decay function formula is given as follows

$$\begin{aligned} G &= 1.0 - 0.0625 \cdot (R)^2, \qquad |R| < 2.0, \\ &= \frac{2}{|R|} - \frac{1}{(R)^2}, \qquad |R| \geqslant 2.0, \end{aligned} \tag{30}$$

for spatial decay function (G_j):

$$G = G_j, \qquad R = R_j, \tag{31}$$

for time-wise decay function (G_t):

$$G = G_t, \qquad R = 4C. \tag{32}$$

The lack of a physical (or mathematical) model for the time decay function does not cause any instability problem because the Eqs. (30)–(32) satisfy the stability criterion (16).

4. Concluding Remarks

Several important conclusions can be made for the present general finite-difference formulation.

(1) The present formulation has been successfully demonstrated to obtain steady-state convergent solution for a square cavity flow and a Couette flow with suction. There is no apparent stability limitation on the grid size and the time step with the present method.

(2) The ability to account for the numerical stability comes from the fact that local analytical model solutions and locally evaluated decay functions are used in the formulations.

(3) Although the present local model was not designed to produce accurate transient solution with large time steps, local models that covered several gridpoints and time steps with a larger region of influence could be developed to provide more accurate transient results.

References

1. C. W. Hirt, *J. Comput. Phys.* **2** (1968), 339.
2. Patrick J. Roache, "Computational Fluid Dynamics," Hermosa, 1972.
3. D. N. De G. Allen and R. V. Southwell, *Q. J. Mech. and Applied Math.* **8** (1955), 129.
4. D. B. Spalding, *Int. J. Num. Meth. Engng.* **4** (1972), 551.
5. O. Burggraf, *J. Fluid Mech.* **24** (1966), 113.
6. R. D. Mills, *J. Roy Aero. Soc.* **69** (1965), 714.
7. A. K. Runchal, D. B. Spalding, and M. Wolfshtein, *Phys. Fluids*, Supplement II, II-21, (1969).
8. D. Greenspan, *Comput. J.* **12** (1969), 89.
9. J. D. Bozeman and C. Dalton, *J. Comput. Phys.* **12** (1973), 348.